

Pollutant Removal from Gaseous and Aqueous Phases using Hydrochar-based Activated Carbon

Monica Puccini*, Eleonora Stefanelli, Andrea Luca Tasca, Sandra Vitolo

Dipartimento di Ingegneria Civile e Industriale, University of Pisa, Largo Lucio Lazzarino 1, 56122 Pisa, Italy
monica.puccini@unipi.it

In this study, hydrochar (HC) produced at industrial scale by hydrothermal carbonization of municipal woody and herbaceous prunings was used for producing activated carbon by KOH chemical activation. Different KOH/HC ratios were studied to produce highly porous materials with high surface area. Activated carbon with a BET surface area up to 1739 m²/g was obtained for a 3:1 KOH/HC ratio. Adsorption properties of obtained samples were studied for removing pollutants both from gas and liquid phases. Thermogravimetric analyzer (TGA) was used for evaluating the removal capacities of CO₂ from a gaseous phase, while UV-Vis spectroscopy was used for evaluating the removal capacities of an emerging contaminant from an aqueous phase. All samples showed a good CO₂ adsorption capacity at 27 °C, reaching 84.5 mg CO₂/g sorbent for hydrochar activated with an impregnation ratio of 2:1. Moreover, activated chars exhibited a high removal efficiency (up to 97.9 % for a 3:1 KOH/HC ratio) for atrazine, which is one of the most common pesticides detected in superficial and groundwater aquifers.

1. Introduction

In view of the growing concern about environmental sustainability, biomass plays an essential role in both energy and materials production. In this context, hydrothermal carbonization (HTC) is a thermo-chemical conversion technology for recovery and enhancement of biomass and organic waste, which is attractive since it offers low-cost, low temperature, environmentally friendly production of novel carbon materials from natural precursors without the need to use toxic chemicals (Wei et al., 2011).

HTC occurs at temperatures between 180 and 250 °C in a biomass-water mixture under self-generated pressure

(up to 2 MPa) for one to twelve hours, resulting in the formation of three main products: solid particles (hydrochar), liquid (bio-oil mixed with water) and small fractions of gases (mainly CO₂) (Bamdad et al., 2018).

Hydrochar exhibits a carbonaceous matrix and it could be employed as fuel and in several fields, such as agriculture, horticulture (Puccini et al., 2018), manufacturing of materials (electrodes, or composites). The high content of oxygenated functional group makes the hydrochar an effective precursor for the production of chemically activated carbon (Jain et al., 2016).

Several studies are focused on the production of activated carbons from hydrothermally treated biomasses, like rye straw (Falco et al., 2013), corncob (Arellano et al., 2016), rice husk (Ding et al., 2013), coconut shells (Jain et al., 2015), and sawdust (Sevilla et al., 2017). Activation of these precursors results in formation of highly porous activated carbons, whose large surface areas facilitate their performance as adsorbents. High porosity is extremely desirable for enhanced performance of adsorbents, since it facilitates high mass transfer and adsorbate loading (Jain et al., 2016). Varying activation conditions (such as temperature, type and concentration of activating agent) influence the textural properties of obtained activate carbons, making them suitable for different applications including energy storage in capacitors (Ding et al., 2013; Sevilla et al., 2017) and CO₂ capture (Sevilla et al., 2012; Sevilla and Fuertes, 2011).

Another recent field of application for activated carbons derived from hydrothermally treated biomasses is the removal of organic and inorganic pollutants from aqueous solutions (Han et al., 2017; Liu et al., 2016). Many studies on biochar produced by thermal degradation of biomasses have shown good performances in

adsorption of pesticides, as triazine herbicides (atrazine, simazine, terbuthylazine) which are frequently detected in high concentrations in surface and groundwater (Tasca et al., 2018; Mandal et al., 2017).

In this study, activated carbons were prepared by KOH chemical activation of hydrochar obtained from hydrothermal carbonization of green waste. The concentration of activating agent was varied in order to produce high surface area activated carbon. Obtained activated chars were characterized in terms of their morphology and porous structure (specific surface area and micropore volume). Their adsorption ability was studied for CO₂ in gaseous phase, and for an emerging contaminant (atrazine) in aqueous phase.

2. Experimental

2.1 Materials

Hydrochar from HTC treatment of green waste (GW-HC), supplied by Ingelia Srl (Valencia), was used as precursor for the preparation of activated carbon. Potassium hydroxide (KOH - Sigma Aldrich Co. Llc, Analytical grade chemicals) was used as chemical activating agent. Atrazine (PESTANAL, Analytical standard, Sigma Aldrich Co. Llc) was selected as herbicide for sorption analyses in aqueous phase.

2.2 Activated carbon preparation and characterization

GW-HC was first dried at 105 °C for 24 h and ground in an agate mortar for 3 hr. Then, the obtained powders were sieved to particle size less than 75 µm. Chemical activation of hydrochar with KOH was carried out at 600 °C for 1 h under nitrogen atmosphere, according to the procedure reported in our previous work (Puccini et al., 2017). Different KOH/HC impregnation ratios (weight terms) were studied ranging from 1:1 to 4:1. Activated char samples were then mixed with HCl 5 M, washed with deionized water until they reached a pH of 7, and finally dried at 105 °C for 15 h. HCl solution was used for cleaning and removing residual reagents. Activated chars were denoted as GW-AC_x, where x indicated the KOH/HC ratio used for the synthesis.

Proximate analysis of GW-HC and activated chars was carried out by using a thermogravimetric analyzer (TGA Q500 TA Instruments). For the determination of moisture and volatile matter, 12 ± 1 mg of sample were weighed and heated from 30 to 900 °C at 20 °C/min, under nitrogen flow (100 vol%). Then, the sample was cooled down from 900 to 800 °C and C and the flow was switched to air for the determination of fixed carbon and ash.

Specific surface area of activated char samples was determined by physical adsorption of N₂ at different pressures at -196 °C using an automatic adsorption system (NOVA 1200e Quantachrome Instruments). The specific surface area was calculated by the Brunauer-Emmett-Teller (BET) equation (Brunauer et al., 1938) from the adsorption data obtained in the relative pressure (P/P₀) range of 0.05 to 0.3. The micropore volume was estimated according to the Horvath-Kawazoe (HK) method (Horvath and Kawazoe, 1983), while the average pore diameter was calculated using the density functional theory (DFT) method (implemented into Quantachrome's data software) using nitrogen adsorption data.

The shapes and morphology of activated chars were also observed by using a JEOL 5600LV Scanning Electron Microscope (SEM). The samples were coated with Au on a SEM coating device (Edwards Sputter Coater S150B) to induce electro conductivity. A homogeneous layer of metal of 5-6 nm thickness coated the entire sample surface.

2.3 Adsorption studies

Adsorption capacity of activated chars obtained from GW-HC was tested in both gaseous and aqueous phases. Carbon dioxide and atrazine were selected as adsorbates. CO₂ adsorption tests were performed using a thermogravimetric balance. The sample (12 ± 1 mg) was placed in a platinum sample pan and first heat-treated at 105 °C for 1 h under a nitrogen flow of 100 mL/min. Subsequently, the sample was cooled down to 27 °C and the N₂ flow was switched to a CO₂/N₂ mixture containing 60 vol% of CO₂. The total feed gas flow rate was maintained at 100 mL/min at atmospheric pressure. The weight increase during the isothermal CO₂ adsorption process, lasted 20 min, was recorded as a function of time.

Batch adsorption experiments were performed to test the interaction between activated chars and atrazine for applying activated GW-HC as a sorbent for the herbicide. 2 mg of activated GW-HC were placed in contact with 20 mL of an atrazine solution with an initial concentration of 10 mg/L and kept for 1h in a shaker at room temperature (approximately 20 °C). Then, the residual atrazine concentration was measured by UV-Vis spectrophotometer Shimadzu UV-1700 PharmaSpec at 223 nm. Pesticide removal efficiency was calculated by the Eq(1):

$$\% \text{ Removal} = \frac{(C_0 - C_e)}{C_0} \cdot 100 \quad (1)$$

where C₀ and C_e are the initial and equilibrium concentration of atrazine solution in mg/L, respectively.

3. Results and discussion

3.1 Activated carbon characterization

The proximate analysis of raw and activated hydrochar is reported in Table 1. The results show substantial changes in volatile matter and fixed carbon between GW-HC and GW-ACs. As expected, after activation at 600 °C, the content of volatile matter decreases from 63.72 to 15.47 % of GW-AC1, and slightly increase with increasing the KOH/HC ratio. The amount of fixed carbon increases from 18.70 to values above 65 % except for GW-AC4, which shows a lower content of fixed carbon (40.32 %) and a content of ashes over two times than activated hydrochars with a lower impregnation ratio.

Table 1: Proximate analysis of hydrochar from green waste (GW-HC) and activated chars (GW-ACs).

Sample	Volatile matter (wt%)*	Ashes (wt%)*	Fixed carbon (wt%)*
GW-HC	63.72	17.58	18.70
GW-AC1	15.47	16.71	67.82
GW-AC2	16.32	14.68	69.00
GW-AC3	20.99	12.75	66.26
GW-AC4	23.80	35.88	40.32

* dry basis

The SEM images describe the morphologies of GW-ACs derived from hydrochar (Figure 1). Although micropores and mesopores are not visible, the shape and location of macropores can be observed. All activated chars present a porous structure, with larger pores as the KOH/HC ratio increases. Sample GW-AC1 (Figure 1a) presents a non-complete porosity; this could be due to a non-uniform distribution of activating agent with hydrochar when KOH/HC ratio is 1. Whereas, samples GW-AC2 and GW-AC3 (Figures 1b and 1c) display a more uniform porous structure owing to a higher amount of KOH used for activation. However, an impregnation ratio of 4 (Figure 1d) leads to a fragmented structure with macropores of very large dimensions.

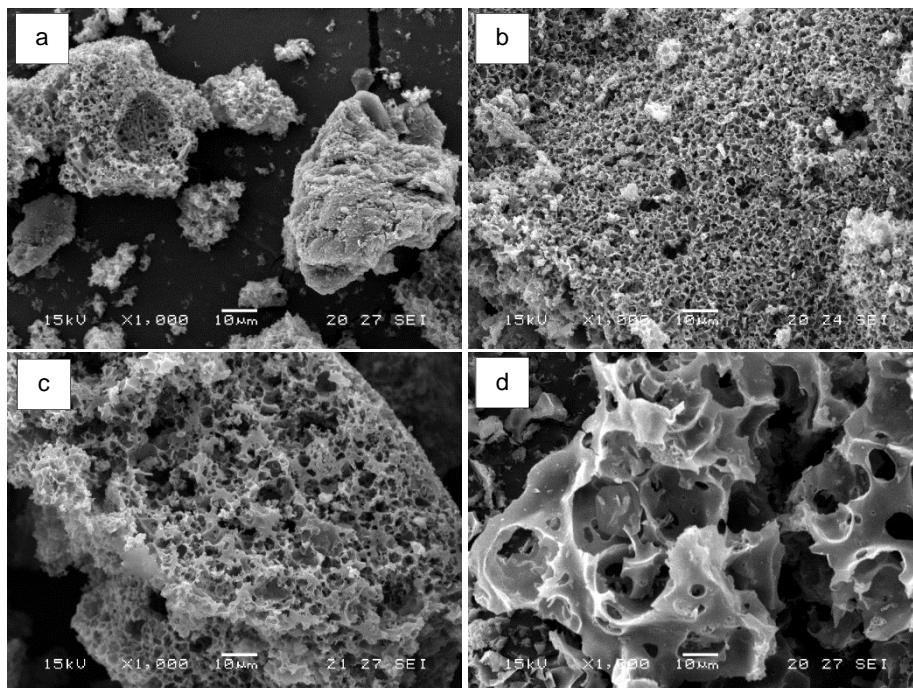


Figure 1: SEM images of GW-HC after chemical activation: (a) GW-AC1 (1:1 KOH/HC ratio); (b) GW-AC2 (2:1 KOH/HC ratio); (c) GW-AC3 (3:1 KOH/HC ratio); (d) GW-AC4 (4:1 KOH/HC ratio).

In order to characterize the porosity of activated chars, N₂ adsorption at -196 °C was conducted for all GW-ACs samples. N₂ adsorption/desorption isotherms are shown in Figure 2; the textural characteristics of activated chars are reported in Table 2. All the N₂ isotherms of activated samples are characterized by a Type I profile, with a more or less pronounced knee depending on the activation conditions. The steep adsorption of

N₂ at very low relative pressure ($P/P_0 < 0.1$) indicates a microporous structure of these materials, which is confirmed by high BET surface area and average pore diameter values below 2 nm. Increasing the KOH/HC ratio from 1 to 3 leads to activated chars with higher surface area (from 839 to 1739 m²/g) and micropore volume (from 0.38 to 0.86 cm³/g); whereas GW-AC4 surface area (1409 m²/g) and micropore volume (0.68 cm³/g) are lower than GW-AC3 values. These results are in agreement with SEM images, which show the presence of a fragmented structure with large macropores for sample GW-AC4 (Figure 1d). Unlike the higher surface area and micropore volume obtained for samples with higher KOH/HC ratio (3 and 4), the sample GW-AC2 exhibits the lowest average pore size (1.1 nm) likely related to a narrow-size microporous structure. Therefore, a porous structure with narrow micropores depends on hydrochar degree of activation (KOH/HC ratio).

As described in previous work (Puccini et al., 2017), the development of porosity is related to the reaction of KOH with C under inert conditions, leading to the formation of different potassium species (K₂O, K, K₂CO₃) during the activation step. The diffusion of these species within hydrochar structure widens existing pores, leading to a well-developed micropore structure up to a 3:1 KOH/HC ratio. When the impregnation ratio increases to 4, the porous structure breaks up due to the high amount of activating agent, resulting in an enlargement of the porosity and a decrease of both the surface area and micropore volume.

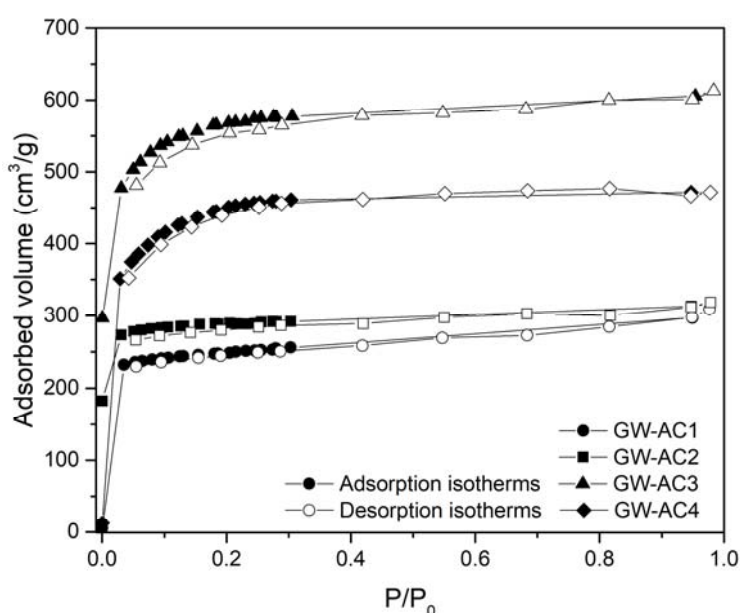


Figure 2: N₂ adsorption and desorption isotherms of activated hydrochars.

Table 2: BET surface area and porosity results of activated chars (GW-ACs).

Sample	BET surface area (m ² /g)	Micropore volume ^a (cm ³ /g)	Average pore diameter ^b (nm)
GW-AC1	763.71	0.38	1.4
GW-AC2	839.40	0.43	1.1
GW-AC3	1739.27	0.86	1.5
GW-AC4	1409.42	0.68	1.4

^a Evaluated by the HK method.

^b Calculated by the DFT method.

3.2 Adsorption experiments

The CO₂ adsorption capacities of GW-HC and GW-ACs were investigated by TGA at atmospheric pressure (1 bar) and 27 °C under a CO₂/N₂ mixture of 60/40 vol% (Figure 3). As shown, raw hydrochar displays a very low CO₂ adsorption capacity, about 0.1 mmol CO₂/g (4.9 mg CO₂/g sorbent). KOH activation improves significantly the CO₂ uptake, that increases with increasing the KOH/HC ratio from 1 to 2, reaching 1.9 mmol CO₂/g (84.5 mg CO₂/g sorbent). Whereas, for samples GW-AC3 and GW-AC4 the CO₂ adsorption capacity decreases. Although the porous carbon prepared with 2:1 KOH/HC ratio has a lower porosity development than those obtained with higher KOH/HC ratio (3 and 4) (see Table 2), it exhibits significantly better CO₂ capture capacity.

This behavior is likely due to the major contribute of narrow-size micropores. Indeed, GW-AC2 sample presents micropores with average pore diameter of 1.1 nm, which give a greater contribution to CO₂ adsorption than wide micropores and mesopores, since narrow micropores have strong adsorption potentials that enhance their filling by the CO₂ molecules (Sevilla and Fuertes, 2011).

Adsorption behavior of atrazine from aqueous solutions on activated hydrochars was studied by carrying out batch experiments with atrazine initial concentration of 10 mg/L. Pesticide removal efficiencies for all GW-ACs are reported in Table 3. The experimental results show that the lowest percentage removal is obtained using GW-HC activated with 1:1 KOH/HC ratio, while 97.9 % of removal is reached increasing the KOH/HC ratio to 3. When impregnation ratio is 4 a reduction in atrazine adsorption is observed, decreasing to a value of 73.0 %. The obtained results highlight the correlation among the adsorption capacity of GW-ACs and their porosity: activated chars having the highest surface area and micropore volume present the highest value of atrazine removal from aqueous medium. Sample GW-AC2, which shows the best CO₂ uptake, has by contrast a low atrazine removal efficiency (35.3 %). This is likely due to the presence of narrow-size micropores, which hinder atrazine adsorption due to its molecular dimension (Pelekani and Snoeyink, 2000).

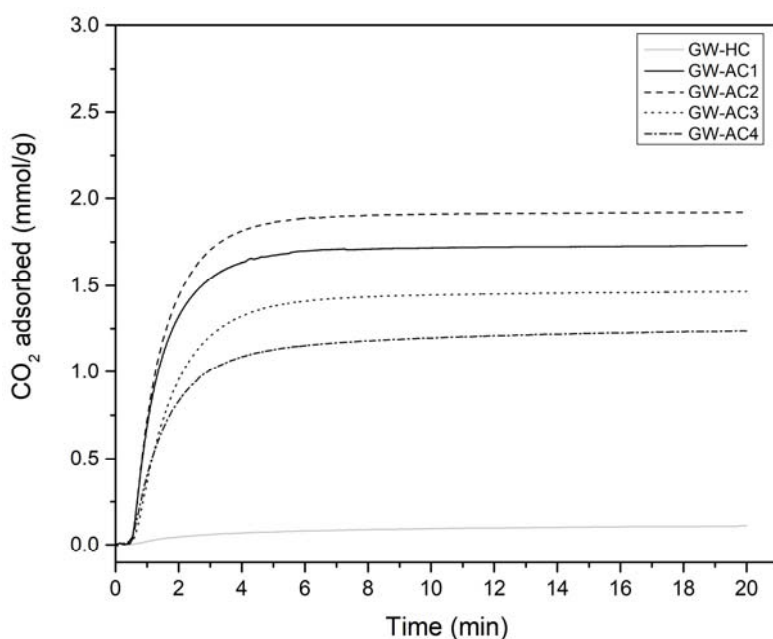


Figure 3: CO₂ adsorption at 27 °C and 1 bar (60 vol% of CO₂) of raw and activated hydrochars.

Table 3: Atrazine removal efficiency of activated chars (GW-ACs).

Sample	% Removal
GW-AC1	24.6
GW-AC2	35.3
GW-AC3	97.9
GW-AC4	73.0

4. Conclusions

Sustainable porous carbons were prepared from hydrothermally treated green waste by activation using KOH as activating agent. Activated hydrochars presented high specific surface area and a microporous structure with average pore size less than 2 nm. The application of activated chars as adsorbents for pollutants in both gaseous and aqueous phases was studied. A KOH/HC ratio of 2 allowed to obtain activated chars with good CO₂ adsorption performances at room temperature (84.5 mg CO₂/g sorbent at 27 °C and 1 bar). This capacity is likely due to a major contribute of narrow-size micropores (1.1 nm). Experimental results confirmed also the presence of interactions between activated hydrochar and atrazine. The removal efficiency of atrazine from water solution is strongly correlated to the surface area of the sorbent, with 97.9 % of removal attainable using hydrochar activated with a 3:1 KOH/HC ratio. The present work suggests that an activated carbon can be

obtained from the valorization of solid wastes and its high adsorption efficiency suggests its application as a novel, competitive adsorbent for atrazine.

References

- Arellano O., Flores M., Guerra J., Hidalgo A., Rojas D., Strubinger A., 2016, Hydrothermal carbonization of corncob and characterization of the obtained hydrochar, *Chemical Engineering Transactions*, 50, 235–240.
- Bamdad H., Hawboldt K., MacQuarrie S., 2018, A review on common adsorbents for acid gases removal: Focus on biochar, *Renewable and Sustainable Energy Reviews*, 81, 1705–1720.
- Brunauer S., Emmett P.H., Teller E., 1938, Adsorption of Gases in Multimolecular Layers, *Journal of the American Chemical Society*, 60, 309–319.
- Ding L., Zou, B., Li Y., Liu H., Wan, Z., Zhao C., Su Y., Guo Y., 2013, The production of hydrochar-based hierarchical porous carbons for use as electrochemical supercapacitor electrode materials, *Colloids and Surfaces A: Physicochemical and Engineering Aspects*, 423, 104–111.
- Falco C., Marco-Lozar J.P., Salinas-Torres D., Morallón E., Cazorla-Amorós D., Titirici M.M., Lozano-Castelló D., 2013, Tailoring the porosity of chemically activated hydrothermal carbons: Influence of the precursor and hydrothermal carbonization temperature, *Carbon*, 62, 346–355.
- Han L., Sun H., Ro K.S., Sun K., Libra J.A., Xing B., 2017, Removal of antimony (III) and cadmium (II) from aqueous solution using animal manure-derived hydrochars and pyrochars, *Bioresource Technology*, 234, 77–85.
- Horvath G., Kawazoe K., 1983, Method for the calculation of effective pore size distribution in molecular sieve carbon, *Journal of Chemical Engineering of Japan*, 16, 470–475.
- Jain A., Balasubramanian R., Srinivasan M.P., 2016, Hydrothermal conversion of biomass waste to activated carbon with high porosity: A review, *Chemical Engineering Journal*, 283, 789–805.
- Jain A., Balasubramanian R., Srinivasan M.P., 2015, Production of high surface area mesoporous activated carbons from waste biomass using hydrogen peroxide-mediated hydrothermal treatment for adsorption applications, *Chemical Engineering Journal*, 273, 622–629.
- Liu B., Li Y., Gai X., Yang R., Mao J., Shan S., 2016, Exceptional adsorption of phenol and p-nitrophenol from water on carbon materials prepared via hydrothermal carbonization of corncob residues, *BioResources*, 11, 7566–7579.
- Mandal A., Singh N., Purakayastha T.J., 2017, Characterization of pesticide sorption behaviour of slow pyrolysis biochars as low cost adsorbent for atrazine and imidacloprid removal, *Science of The Total Environment*, 577, 376–385.
- Pelekani C., Snoeyink V.L., 2000, Competitive adsorption between atrazine and methylene blue on activated carbon: the importance of pore size distribution, *Carbon*, 38, 1423–1436.
- Puccini M., Stefanelli E., Hiltz M., Seggiani M., 2017, Activated Carbon from Hydrochar Produced by Hydrothermal Carbonization of Wastes, *Chemical Engineering Transactions*, 57, 169–174.
- Puccini M., Ceccarini L., Antichi D., Seggiani M., Tavarini S., Latorre M.H., Vitolo S., 2018, Hydrothermal carbonization of municipal woody and herbaceous prunings: hydrochar valorisation as soil amendment and growth medium for horticulture, *Sustainability*, 10, 846–862.
- Sevilla M., Falco C., Titirici M.M., Fuertes, A.B., 2012, High-performance CO₂ sorbents from algae, *RSC Advances*, 2, 12792–12797.
- Sevilla M., Ferrero G.A., Fuerte A.B., 2017, Beyond KOH activation for the synthesis of superactivated carbons from hydrochar, *Carbon*, 114, 50–58.
- Sevilla M., Fuertes A.B., 2011, Sustainable porous carbons with a superior performance for CO₂ capture, *Energy & Environmental Science*, 4, 1765–1771.
- Tasca A.L., Puccini M., Fletcher A., 2018, Terbutylazine and desethylterbutylazine: Recent occurrence, mobility and removal techniques, *Chemosphere*, 202, 94–104.
- Wei L., Sevilla M., Fuertes A.B., Mokaya R., Yushin G., 2011, Hydrothermal carbonization of abundant renewable natural organic chemicals for high-performance supercapacitor electrodes, *Advanced Energy Materials*, 1, 356–361.